

## Co-Cr FILMS FOR PERPENDICULAR RECORDING

T. Wielinga and J.C. Lodder

**Abstract** - Co-Cr films were prepared by means of RF-sputtering. The dependence of the magnetic parameters on the sputter conditions was investigated. It was found that for increasing Ar-pressure the c-axis of the hcp-structure gradually declines from normal to in-plane orientation. An optimum for the sputter voltage is found. The coercivity increases with decreasing target-substrate distance and this is probably due to surface heating by electron bombardment from the Ar-plasma. The recording characteristics of these Co-Cr films were then investigated by means of stand-still recording experiments. A 6.7  $\mu\text{m}$  thick permalloy single-pole head (SPH) was used for creating a head print in a 1  $\mu\text{m}$  thick Co-Cr layer. The flux reversals are detected by means of a magneto-resistive transducer (MRT). The response was analyzed, using an analytical method for calculating the magnetization distribution in the Co-Cr layer. For this purpose the head field of the SPH was also determined with the same MRT.

## INTRODUCTION

Recently a new interest in perpendicular magnetic recording has started<sup>1,2,3</sup>. This is mainly due to the development of the alloy film Co-Cr which shows favourable characteristics for the perpendicular magnetization mode, i.e. strong perpendicular anisotropy, high coercivity and single-domain behaviour suitable for the preferred rotational reversal mechanism. We deposited Co-Cr layers by means of RF-sputtering and investigated the influence of the sputter parameters on the magnetic and crystallographic properties. The most important parameters are: Argon pressure  $P_{\text{Ar}}$ , sputtering voltage  $V_{\text{RF}}$ , substrate-holder temperature  $T_{\text{sh}}$  and new the target-substrate distance  $d_{\text{ts}}$ .

The perpendicular magnetization mode in Co-Cr films was investigated by means of stand-still recording experiments using a 6.7  $\mu\text{m}$  thick permalloy single-pole head (SPH). We calculated the magnetization pattern in the Co-Cr layer generated by this head, using an analytical model<sup>6</sup> similar to that developed by v. Herk and Wesseling<sup>7</sup>. The magnetization reversals were measured by means of a magneto-resistive transducer (MRT) and the MRT-response compared with that, calculated according to this model. For this purpose knowledge of the field structure of the SPH was required. Therefore the SPH field was analyzed with the same MRT.

## RF-SPUTTERING OF Co-Cr FILMS

RF-sputtering as a deposition method was chosen because of its superiority in adhesion and reproducibility compared with evaporation. The background pressure of the turbomolecular vacuum system was better than  $2 \cdot 10^{-7}$  Torr. We used a 10 cm diameter multi-target, consisting of a Co (99,9%) base plate covered with 13 Cr (99,99%) subtargets (using epoxy) to a surface ratio of 17,5% Cr. We varied the following sputter conditions: Argon (99,998%) pressure  $P_{\text{Ar}}$ , RF-voltage  $V_{\text{RF}}$ , target-substrate distance  $d_{\text{ts}}$  and substrate holder temperature  $T_{\text{sh}}$ .

The latter was measured with a chromel-alumel thermocouple positioned in the substrate holder about 2 mm underneath the 0.3 mm thick silicon substrate. The composition and the thickness of the Co-Cr films were determined by means of X-ray fluorescence. Despite the varying experimental conditions the resulting film composition was almost constant (17 to 19 at% Cr) due to the similar sputter yields of Co and Cr. The deposition rate was 2  $\text{\AA}/\text{s}$  at  $V_{\text{RF}} = 1,50$  kV,  $P_{\text{Ar}} = 3$  m Torr and  $d_{\text{ts}} = 50$  mm. The homogeneity of the films was established by microprobe analysis. The crystallographic structure was measured by X-ray diffraction. It is found that a hcp-structure is formed. The c-axis orientation is measured by means of the rocking technique. The magnetic parameters, i.e. the saturation magnetization  $M_{\text{S}}$ , the perpendicular coercivity field strength  $H_{\text{C}}^{\perp}$  and remanence  $S_{\perp} (= M_{\text{r}}/M_{\text{S}})$  plus their inplane equivalents  $H^{\parallel}$  and  $S_{\parallel}$  are measured by means of a vibrating sample magnetometer (V.S.M.).  $M_{\text{S}}$  is 650 Gs for 17 at% Cr, about 40% more than found by Iwasaki and Ouchi<sup>4</sup>. This relative large difference may be due to the strong composition dependence of the magnetization in this range.

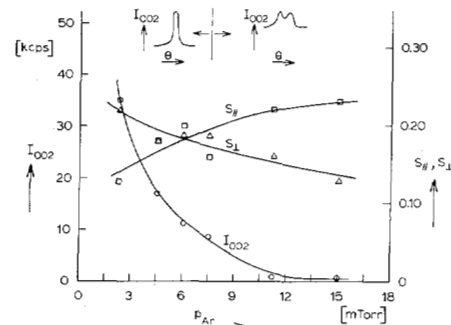


Fig. 1: The dependence of  $S_{\perp}$ ,  $S_{\parallel}$ , and  $I_{002}$  on  $P_{\text{Ar}}$ ;  $h \approx 1 \mu\text{m}$ ,  $V_{\text{RF}} \approx 1.50$  kV,  $d_{\text{ts}} = 5$  cm and  $T_{\text{sh}} \approx 160^{\circ}\text{C}$ .

In Fig. 1 the dependences of  $S_{\perp}$ ,  $S_{\parallel}$ , and  $I_{002}$ , the intensity of the 002-reflection normal to the film surface, on  $P_{\text{Ar}}$  are shown. The lower limit of the  $P_{\text{Ar}}$  range is the ultimate limit for a stable Ar plasma. No maximum is found for  $S_{\perp}$ ,  $S_{\parallel}$ , or  $I_{002}$ . With increasing  $P_{\text{Ar}}$ , the magnetic and crystallographic quality decreases, which is demonstrated by an increasing deviation from the normal of the c-axis for  $P_{\text{Ar}}$  above 7.5 m Torr as shown by the rocking curves (see inset); with increasing  $P_{\text{Ar}}$  the intensity  $I_{002}$  decreases together with strong broadening of the line and the half angle width  $\Delta\theta$  increases from  $5^{\circ}$  to  $15^{\circ}$ . When  $P_{\text{Ar}}$  is more than about 7.5 m Torr, the  $I_{002}$ -line splits up into two sublines with slightly increasing angle distance from  $10^{\circ}$  to  $20^{\circ}$ .

It can be concluded, that at low argon pressures ( $P_{\text{Ar}} < 7.5$  m Torr) the hcp Co-Cr film has a pronounced  $\langle 002 \rangle$  orientation, which deteriorates for increasing  $P_{\text{Ar}}$ . Iwasaki and Ouchi<sup>4</sup> also used a relative low argon pressure (10 m Torr).

In Fig. 2 the dependences of  $H_{\text{C}}^{\perp}$  and  $S_{\parallel}$  on  $V_{\text{RF}}$  are presented. For both values of  $d_{\text{ts}}$  the  $H_{\text{C}}^{\perp}$  "saturates" at  $V_{\text{RF}}$  about 1.50 kV and also at this sputter voltage a minimum is found for  $S_{\parallel}$ . It is noticeable that  $H_{\text{C}}^{\perp}$  is different for the various  $d_{\text{ts}}$  and strongly increases with increasing  $V_{\text{RF}}$ . In order to examine these features somewhat further, we varied the target-substrate distance  $d_{\text{ts}}$ . These results are presented in Fig. 3, and show an increasing  $H_{\text{C}}^{\perp}$  and  $S_{\perp}$  for decreasing  $d_{\text{ts}}$ .

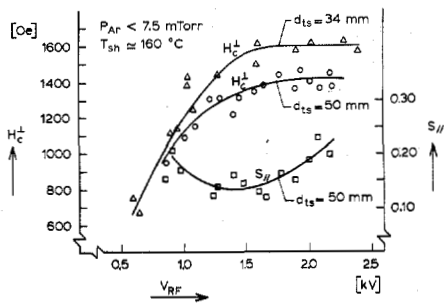


Fig. 2: The dependence of  $H_C$  and  $S_{||}$  on  $V_{RF}$ ;  $h \approx 1 \mu m$ ,  $P_{Ar} < 7.5 \text{ m Torr}$ ,  $T_{sh} = 160^\circ C$  and  $d_{ts} = 34$  and  $50 \text{ mm}$ .

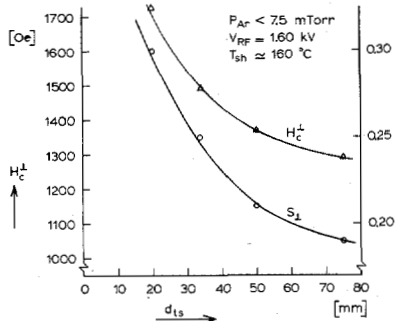


Fig. 3:  $H_C^perp$  and  $S_{\perp}$  as a function of  $d_{ts}$ ;  $V_{RF} = 1.60 \text{ kV}$ ,  $P_{Ar} < 7.5 \text{ m Torr}$  and  $T_{sh} \approx 160^\circ C$ .

Figure 4 shows an increasing  $H_C^perp$  and a decreasing  $I_{002}$  with increasing  $T_{sh}$ . For  $T_{sh} \geq 240^\circ C$  the  $I_{002}$  rocking curve shows line splitting like in Fig. 1.

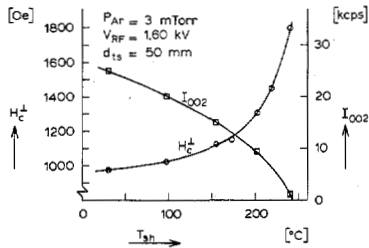


Fig. 4: The  $H_C^perp$  - and  $I_{002}$ -dependence on  $T_{sh}$ .

The noticeable features of Fig. 2 can now be explained on the basis of surface heating of the substrate by electron bombardment from the Ar-plasma. Because of the induced temperature gradient in the substrate holder, the surface temperature can be much higher than the measured temperature  $T_{sh}$ . It is also well known, that heating by electron bombardment increases with decreasing  $d_{ts}$ . The difference in  $H_C^perp$  for  $d_{ts} = 34$  resp.  $50 \text{ mm}$  may therefore be explained by different surface temperatures. The increase of  $H_C^perp$  with increasing  $V_{RF}$  may be explained by the increasing surface temperature with increasing  $V_{RF}$ . This is clearly demonstrated by line splitting of the rocking curves for  $V_{RF} > 1.50 \text{ kV}$  as was observed for  $T_{sh} \geq 240^\circ C$  in Fig. 4. For  $V_{RF} > 1.50 \text{ kV}$   $H_C^perp$  shows no further increase but remains almost constant. The reason for this is not quite clear; however, secondary effects as re-emission may also have some influence at a high sputtering voltage. It is also concluded, that the coercivity is mainly determined by the substrate temperature and less by the crystallographic orientation. Because the structural features are strongly influenced by the substrate temperature<sup>8</sup>, it is assumed that the film structure is the dominant factor for the coercivity. Furthermore, the dependences of  $S_{||}$ ,  $S_{\perp}$  and  $H_C^perp$  on  $V_{RF}$ , as shown in Fig. 2, suggest that  $V_{RF}$  is the primary

factor rather than the growth rate  $R$ , because the same optimal  $V_{RF}$  is found for  $d_{ts} = 34$  and  $50 \text{ mm}$ , while the difference in  $R$  is about 50%.

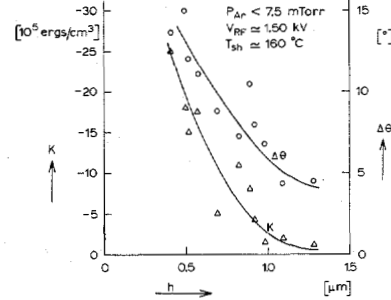


Fig. 5: The anisotropy  $K$  and the half angle width  $\Delta\theta$  as a function of the film thickness.

Finally in Fig. 5 the effective anisotropy  $K (= K_u - 2\pi M_s^2)$ , measured with a torque magnetometer and the rocking curve half angle width  $\Delta\theta$  are shown. It is suggested from this figure, that the intrinsic anisotropy  $K_u$  is rather small in thin films and only reaches its maximum for  $h \geq 1 \mu m$ . This suggestion is supported by the decrease of  $\Delta\theta$  with increasing  $h$ , indicating the crystalline origin of the magnetic anisotropy. As shown in Fig. 5 the effective anisotropy  $K$  is almost zero or just negative and with  $M_s = 650 \text{ (emu/cm}^3\text{)}$  the intrinsic anisotropy  $K_u$  is about  $+ 25 \cdot 10^5 \text{ (erg/cm}^3\text{)}$ . However, the condition  $K > 0$  for perpendicular magnetization is not stringent, because  $2\pi M_s^2$  is the demagnetization energy density of a single domain plate and in practice the recording medium lowers its magnetization by the strong perpendicular demagnetization as shown by the perpendicular and in-plane hysteresis loops in Fig. 6.

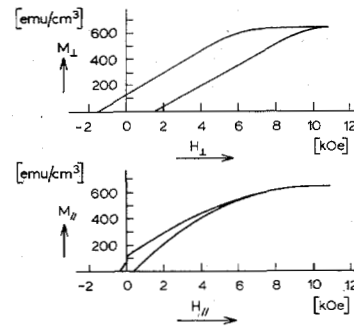


Fig. 6: The perpendicular and in-plane hysteresis of a  $1 \mu m$  thick Co-Cr film, measured by means of a VSM.

The jump in  $M_{||}$  near remanence is probably caused by the reversal of the initial layer ( $\approx 500 \text{ \AA}$ ) at the substrate; thin Co-Cr films of about  $500 \text{ \AA}$  showed considerable in-plane orientation of the c-axis and consequently their perpendicular and in-plane hysteresis loops demonstrated in-plane magnetization.

STAND-STILL RECORDING EXPERIMENTS

In order to obtain insight into the recording characteristics of Co-Cr layers, we performed various stand-still recording experiments. Although the information obtained from this type of experiment is limited, it might provide information about the structure of the flux reversals induced by the single pole head (SPH). A  $1 \mu m$  thick Co-Cr film was first saturated in a strong, perpendicular field ( $\approx 12 \text{ kOe}$ ). A  $6.7 \mu m$  thick permalloy SPH was then placed on the film and activated by a perpendicular field  $H_a$ , anti-parallel to the direction of the initial magnetization in the range of 400 to 1600 Oe. The distance between

the head and the film surface is about 0.5 to 1.0  $\mu\text{m}$ . The flux reversals are analyzed by using a magneto-resistive transducer (MRT) to detect the vertical field component. The equipment used in this experiment is described in the literature<sup>5</sup>. The distance  $z$  between the MRT and the Co-Cr film, and the displacement  $X$  of the MRT along the object, are well-controlled parameters. A bias field  $H_{\text{bias}}$  is applied during the MRT measurement in order to increase its sensitivity (the MRT is a quadratic transducer).

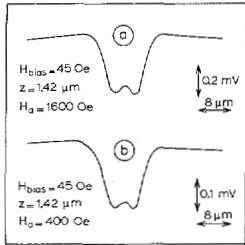


Fig. 7: Several MRT-responses;  $H_{\text{bias}}$  is the field biasing the MRT to increase sensitivity;  $z$  is the MRT to film distance;  $H_a$  was the field, activating the SPH.

The figures 7a and b show the MRT signals of the 6.7  $\mu\text{m}$  SPH print for different values of the activating field  $H_a$ . The responses show qualitative agreement with the results of Potter and Beardsley<sup>2</sup>.

#### SINGLE-POLE HEAD FIELD MEASUREMENTS

The MRT, used in the flux reversal measurements, was also used for the analysis of the vertical head field structure of the 6.7  $\mu\text{m}$  thick permalloy SPH. Our MRT is a permalloy strip with: length  $L = 50 \mu\text{m}$ , width  $w = 2.0 \mu\text{m}$  and thickness  $t = 700 \text{ \AA}$ , placed at the edge of the substratum. Generally speaking the interpretation of the MRT-responses is complicated because of the field gradients across the transducer. In this case however, the thickness of the SPH is relative large compared to the width of the MRT. Therefore in a first order approximation the head field is assumed to be homogeneous across the MRT. The activating field of the head was 4 Oe. Fig. 8a shows some MRT-responses and Fig. 8b shows the derived head fields, in qualitative agreement with the head model measurements of Iwasaki et al<sup>1</sup>. The fields are kept small compared with more realistic values during recording, in order to avoid saturation of the MRT. This means that as yet we have not been able to measure the linearity of the head and its possible saturation effects. This measured head field structure is used for the calculation of its corresponding magnetization reversal induced in the Co-Cr layer.

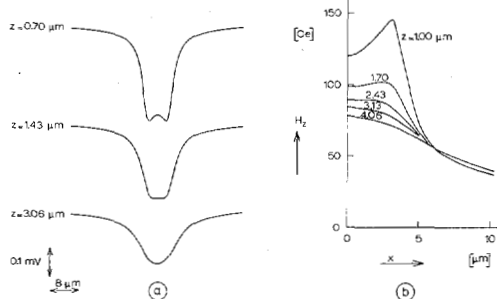


Fig. 8: a) Several MRT-responses of the SPH; the energizing field is 4 Oe;  $z$  is the distance between the SPH and the MRT and b) the calculated SPH field according Fig. 8a;  $z$  is the distance to the SPH surface.

#### FLUX REVERSAL CALCULATIONS

As can be seen from figures 7 and 8a there is a strong congruence between the MRT responses of the SPH field and the created flux reversal. In order to elucidate this point, we calculated the magnetization pattern in the Co-Cr layer which was induced by the SPH field by using a model<sup>6</sup>, analogous to that developed by v. Herk and Wesseling<sup>7</sup>.

In this model only vertical magnetization is assumed and head recording layer interactions are neglected, because in this case the head field ( $\approx 1500 \text{ Oe}$ ) is much stronger than the field ( $\approx 100 \text{ Oe}$ ) generated by the flux reversal. The measured, normalized vertical field of the 6.7  $\mu\text{m}$  thick SPH and the corresponding, calculated vertical magnetization pattern are shown in Fig. 9. The magnetization pattern roughly reflects the head field structure. Fig. 10 shows the corresponding calculated MRT-response together with the measured response from Fig. 7b. The agreement is fairly good.

The magnitude of the SPH field and the distance between SPH and Co-Cr layer have been adjusted to give the best fit between the measured and calculated MRT responses of the flux reversal. The adjusted field value at  $x = 0$  is 1470 Oe in Fig. 9.

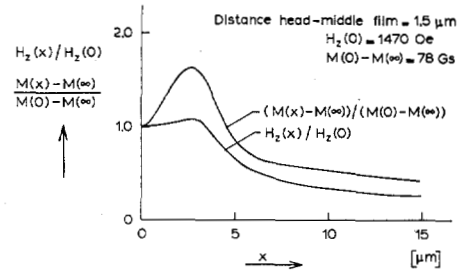


Fig. 9: Normalized SPH field and induced magnetization pattern; the distance between the SPH and the middle of the film is adjusted at 1.5  $\mu\text{m}$ ;  $x = 0$  is the symmetry plane.

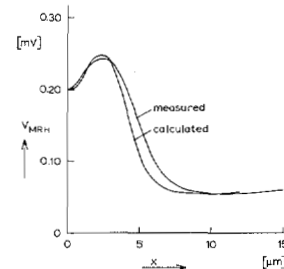


Fig. 10: The measured MRT-response of Fig. 7b and the calculated according the magnetization pattern of Fig. 9.

#### ACKNOWLEDGEMENTS

The authors wish to thank J.H.J. Fluitman, G.H. Jonker and A. van Herk for their stimulating discussions, H.T. Weber for the chemical analysis and H.W.F. Heller for his assistance in the X-ray experimentation.

#### REFERENCES

1. S. Iwasaki, IEEE Trans. Mag., vol. MAG-16, no. 1, 1980.
2. R.I. Potter, I.A. Beardsley, IEEE Trans. Mag., vol. MAG-16, no. 5, 1980.
3. Y. Uesaka, J.H. Judy, 1980 Intermag Conference.
4. S. Iwasaki, K. Ouchi, IEEE Trans. Mag., vol. MAG-14, no. 5, 1978.
5. J.H.J. Fluitman, J.P.J. Groenland, IEEE Trans. Mag., vol. MAG-15, no. 6, 1979.
6. Will be submitted to IEEE Trans. Mag.
7. A. v. Herk, P. Wesseling, IEEE Trans. Mag., vol. MAG-10, no 3, 1974.
8. J.A. Thornton, J. Vac. Sci. Technol., vol. 11, no. 4, 1974.
9. J.H. Keller, R.G. Simmons, IBM J. Res. Develop., vol. 23, no. 1, 1979.